Extended symmetries in geometrical optics

Zhyrair Gevorkian,[1,2] Mher Davtyan,[2] and Armen Nersessian[1,3]
[1]*Yerevan Physics Institute, Alikhanian Brothers St. 2, 0036, Yerevan, Armenia*
[2]*Institute of Radiophysics and Electronics, Ashtarak-2, 0203, Armenia*
[3]*Yerevan State University, 1 Alex Manoogian St., Yerevan, 0025, Armenia*

(Received 2 August 2019; accepted 4 February 2020; published 27 February 2020)

We examine additional symmetries of specific refraction index profiles that are used in the well-known phenomena of perfect imaging and cloaking. In the considered cases, the translation generator and the angular momentum are conserved. We express the ray trajectory parameters through the integrals of motion and observe the existence of a photon state with maximal angular momentum, which can be used as an optical resonator. Application in plasmons and the role of polarization are discussed, and the spin Hall effect in an extended symmetry profile is predicted.

DOI: 10.1103/PhysRevA.101.023840

I. INTRODUCTION

Cloaking phenomena have attracted a great deal of interest since Pendry [1] and Leonhardt [2], who assumed that an object coated by certain inhomogeneous shell becomes invisible to electromagnetic waves. Different mechanisms of cloaking have been suggested since that time, among which are anisotropic metamaterial shells [1], conformal mapping in two-dimensional systems [2], complementary media [3], etc. (for a review see Ref. [4] and references therein). Transformation optics [1] is the most frequently used approach. In this approach, the dielectric permittivity and magnetic permeability tensors are specific coordinate-dependent functions. However, this approach is difficult to implement in the optical field, since it is problematic to find metamaterials with the necessary magnetic properties [5]. In the cases when the photon wavelength is much smaller than the characteristic size of inhomogeneity, geometrical optics approximation is justified [6–9]. In the conformal mapping method of cloaking when geometrical optics approximation is used, closed ray trajectories are of significant importance [2]. Note that these trajectories determine the size and shape of the cloaked area [2].

In the present paper, we thoroughly consider the closed ray trajectories within geometrical optics approximation with the emphasis on the symmetries of the refraction index profile. Namely, we consider the refraction indices, which yield the optical metrics coinciding with those of three-dimensional sphere (for positive κ) and two-sheet hyperboloid (pseudosphere) (for negative κ),

$$n(\mathbf{r}) = \frac{n_0}{|1+\kappa \mathbf{r}^2|}, \quad \kappa = \pm\frac{1}{4r_0^2}. \tag{1}$$

While the generic homogeneous spaces have SO(3) symmetry algebra generated by conserved angular momentum, three-dimensional sphere and pseudosphere have symmetry algebras SO(4) and SO(3.1), respectively. The reason for that is the existence of three additional conserved quantities: translation generators. The two-dimensional counterpart of such refraction index with a positive sign along with other profiles corresponding to the two-dimensional Hamiltonian systems with closed trajectories [2] was already used to describe cloaking phenomena in two dimensions via conformal mapping. This profile is well known in optics as Maxwell's fish eye [10,11] and was debated as a possible tool for perfect imaging [12–14].

In our opinion, the importance of the present consideration is the direct use of extended symmetry of the sphere and pseudosphere. Seemingly, it might be extended to other three-dimensional profiles corresponding to the Hamiltonian systems with close trajectories, such as three-dimensional oscillator and Coulomb potential and their deformations with Calogero-like potentials, as well as their generalizations to three-dimensional spheres and pseudospheres [15]. The consideration of the three-dimensional (two-sheet) hyperboloid, which can be used for the study of plasmon perfect imaging, cloaking is another important point in the given study. Here we have mentioned cloaking and perfect imaging as possible applications of closed ray trajectories. However, there can be other applications too.

In this particular paper, we mostly neglect the light polarization, whose interaction with the inhomogeneity of dielectric permittivity leads to many well-known effects, e.g., the optical Hall effect [16–18], capsize of polarization and straightening of light in dilute photonic crystals [19,20], etc. We only briefly discuss its influence on the trajectories postponing the detailed consideration for the future study.

II. INITIAL RELATIONS

It is well known that minimal action principle came to physics from the geometric optics. Initially, it was invented for the description of the propagation of light in media by Fermat, and is presently known as the Fermat principle,

$$\mathcal{S}_{\text{Fermat}} = \frac{1}{\lambda\!\!\!^{-}_0}\int ds, \quad ds = n(\mathbf{r})|d\mathbf{r}/d\tau|d\tau, \tag{2}$$

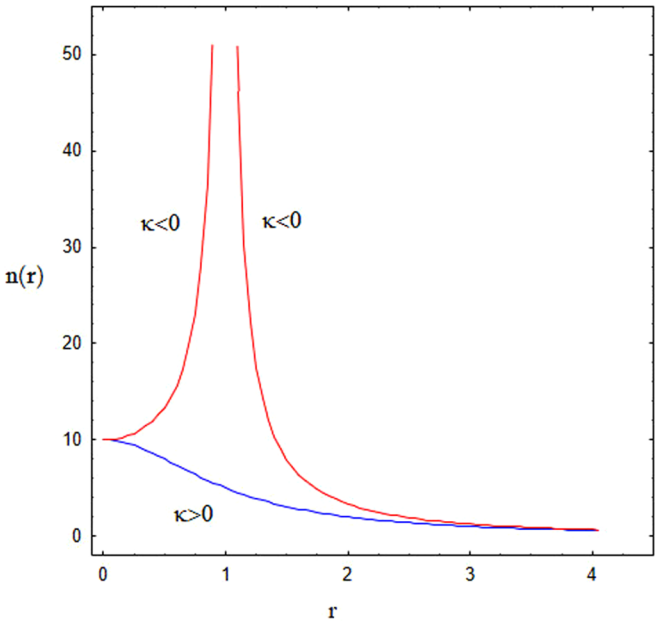

FIG. 1. Refraction index profiles.

where $n(\mathbf{r})$ is the refraction index, and $\lambda\!\!\!^{-}_0$ is wavelength in vacuum, which defines the length of the light trajectory under the assumption that the helicity of light is neglected. This action could be interpreted as the action of the system on the three-dimensional curved space equipped with the optical metrics (or Fermat metrics) of Euclidean signature

$$ds^2 = g_{AB}dx^A dx^B, \quad g_{AB} = n^2(\mathbf{r})\delta_{AB}, \quad A, B = 1, 2, 3. \tag{3}$$

In the special case when the refraction index has a form (1), the Fermat metrics describes three-dimensional sphere (for $\kappa > 0$), or two-sheet hyperboloid (for $\kappa < 0$) with radius r_0. In this case, in addition to rotational, SO(3), symmetry, which yields the conserving angular momentum, the system has SO(4) [SO(3.1)] symmetry, which provides the three-dimensional sphere (hyperboloid), by three additional symmetries conserved quantities. In the case of positive κ, the refraction index is a decreasing function of r, while for the negative κ, it has an increasing part (see Fig. 1). In this paper, we show that due to the extended symmetry mentioned above, these very different profiles lead to closed ray trajectories. As noted in Sec. I, the case of the positive sign was already used to describe cloaking phenomena in two dimensions via conformal mapping [2].

Let us give the Hamiltonian formulation of the system defined by the action (2). Due to its reparametrization invariance, the Hamiltonian constructed by the standard Legendre transformation is identically zero. However, following Dirac's theory [21], the constraint between momenta and coordinates appears as follows:

$$\Phi \equiv g^{ij}(x)p_i p_j - \lambda\!\!\!^{-2}_0 = 0,$$
$$\text{with} \quad g^{ij}p_i p_j = \frac{\mathbf{p}^2}{n^2(\mathbf{r})},$$
$$\text{with} \quad g^{ij}g_{jk} = \delta^i_k. \tag{4}$$

Hence, the Hamiltonian system corresponding to the action (2), is defined by the canonical Poisson brackets

$$\{f, g\} = \frac{\partial f}{\partial x_\alpha}\frac{\partial g}{\partial p_\alpha} - \frac{\partial f}{\partial p_\alpha}\frac{\partial g}{\partial x_\alpha} \tag{5}$$

and by the Hamiltonian

$$\mathcal{H}_0 = \alpha(\mathbf{p}, \mathbf{r})\Phi = \alpha(\mathbf{p}, \mathbf{r})\left(\frac{\mathbf{p}^2}{n^2(\mathbf{r})} - \lambda\!\!\!^{-2}_0\right) \approx 0. \tag{6}$$

Here α is the Lagrangian multiplier, which could be an arbitrary function of coordinates and momenta. When we write down the Hamiltonian equations of motion, the notation "weak zero" ($\mathcal{H}_0 \approx 0$) indicates that we should take into account the constraint (4) only after differentiation,

$$\dot{f}(\mathbf{r}, \mathbf{p}) = \{f, \mathcal{H}_0\} = \{f, \alpha\}\Phi + \alpha\{f, \Phi\} \approx \alpha\{f, \Phi\}. \tag{7}$$

The arbitrariness in the choice of the function α reflects the reparametrization invariance of the action (2). Suppose, for the description of the equations of motion in terms of arc length of the original Euclidian space one should choose (see Ref. [18])

$$\alpha^{-1} = \frac{|\mathbf{p}| + \lambda\!\!\!^{-1}_0 n(\mathbf{r})}{n^2(\mathbf{r})}, \quad \Rightarrow \quad \mathcal{H}_0 = |\mathbf{p}| - \lambda\!\!\!^{-1}_0 n(\mathbf{r}). \tag{8}$$

With this choice, the Hamiltonian equations of motion take the conventional form [22]

$$\dot{\mathbf{p}} = \lambda\!\!\!^{-1}_0 \nabla n(\mathbf{r}), \quad \dot{\mathbf{r}} = \mathbf{p}/|\mathbf{p}|. \tag{9}$$

These equations describe the motion of a wave package with center coordinate $\mathbf{r}$ and momentum $\mathbf{p}$ in a curved space. However, for preserving the similarity with classical mechanics we will deal with the generic formulation (6), i.e., we will not fix the parametrization of light rays.

We are interested in the integrals of motion, i.e., physical quantities that are conserved along the ray trajectory. For the isotropic media, when the refraction index is a spherical symmetric function, $n(\mathbf{r}) = n(|\mathbf{r}|)$, the angular momentum of the system is conserved

$$\mathbf{L} = \mathbf{r} \times \mathbf{p}. \tag{10}$$

When the refraction index has the form (1), the Fermat metrics coincide with those of three-dimensional sphere (for $\kappa > 0$) or two-sheet hyperboloid (for $\kappa < 0$) written in conformal flat coordinates (we ignore here n_0 factor),

$$\frac{d\mathbf{r} \cdot d\mathbf{r}}{\left(1 \pm \frac{\mathbf{r}^2}{4r_0^2}\right)^2} = \left(d\mathbf{y} \cdot d\mathbf{y} \pm dy_4^2\right)|_{y_4^2 \pm \mathbf{y}^2 = r_0^2}, \tag{11}$$

where

$$y_4 = -r_0\frac{1 - \kappa\mathbf{r}^2}{1 + \kappa\mathbf{r}^2}, \quad \mathbf{y} = \frac{\mathbf{r}}{1 + \kappa\mathbf{r}^2}, \quad \text{with} \quad \kappa = \pm\frac{1}{4r_0^2}. \tag{12}$$

From Eq. (12) we get

$$\mathbf{r} = 2r_0\frac{\mathbf{y}}{r_0 + y_4} \;\Rightarrow\; \mathbf{r}^2 = 4r_0^2\frac{r_0 - y_4}{r_0 + y_4}. \tag{13}$$

This is just stereographic projection of the (pseudo)sphere on the $\mathbf{r}$ space, which touches it at the pole $y_4 = -r_0$. The upper

and lower hemispheres are projected to the inside and outside of the three-dimensional ball with radius $2r_0$, respectively. The equatorial sphere $y_4 = 0$ is projected to the boundary of that ball, which is a two-dimensional sphere in the $\mathbf{r}$ space. Due to the SO(4) [SO(3.1)] symmetry of three-dimensional sphere (hyperboloid), in addition to SO(3) algebra generators (10), the system possesses three more conserving quantities

$$\mathbf{T} = (1 - \kappa \mathbf{r}^2)\mathbf{p} + 2\kappa(\mathbf{pr})\mathbf{r} : \{\mathbf{T}, \mathcal{H}_0\} = 0. \tag{14}$$

The Hamiltonian becomes Casimir of SO(4) [SO(3.1)] algebra(s)

$$\frac{\mathbf{p}^2}{(1+\kappa r^2)^2} = \mathbf{T}^2 + 4\kappa \mathbf{L}^2 \;\Rightarrow\; \mathbf{T}^2 + 4\kappa \mathbf{L}^2 = \frac{n_0^2}{\lambda\!\!\!^{-}_0^2}. \tag{15}$$

Notice also, that $\mathbf{T}$ is perpendicular to $\mathbf{L}$: $\mathbf{T} \perp \mathbf{L}$.

III. TRAJECTORIES

Extended symmetry allows to obtain ray trajectories without solving the equations of motion (9). Namely, the vector product of $\mathbf{T}$ and $\mathbf{r}$ immediately yields the expression of trajectories,

$$\mathbf{L} = \frac{\mathbf{T} \times \mathbf{r}}{1 - \kappa \mathbf{r}^2} \;\Rightarrow\; |\mathbf{r} - \mathbf{a}_0|^2 = R_0^2,$$
$$\mathbf{a}_0 \equiv \frac{\mathbf{T} \times \mathbf{L}}{2\kappa L^2}, \quad R_0 = \frac{n_0}{2|\kappa| L \lambda\!\!\!^{-}_0}. \tag{16}$$

Ray trajectories are the circles with center $\mathbf{a_0}$ and radius R_0 [11]. Note that the radius of circle is independent of the sign of κ, whereas the coordinates of the center $\mathbf{a_0}$ depend on the sign of κ. From (16), it is easy to find that

$$|a_0| = \sqrt{R_0^2 - 1/\kappa}. \tag{17}$$

Using expressions (17) and (16) one can draw the ray trajectories Fig. 2. For the photons with zero angular momentum $L = 0$, the radius of the circle goes to infinity $R_0 \to \infty$, i.e., we get a straight line. In contrast with common approaches (see, e.g., Ref. [11]), we express the equations of ray characteristics (16) through the integrals of motion, which allows us to consider different physical situations.

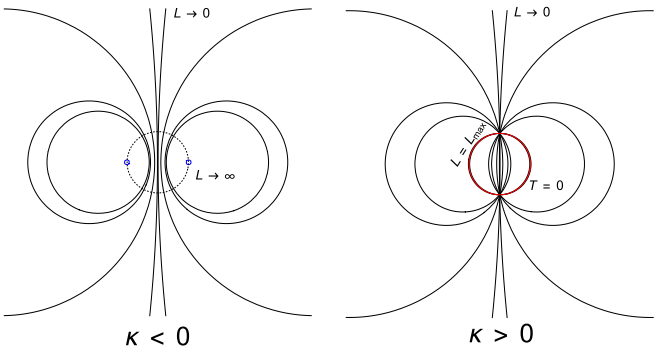

FIG. 2. Ray trajectories for different values of $\mathbf{T}, \mathbf{L}, \kappa$. Dashed and red circles with radius $2r_0$ are given by the refraction profile (1). The red circle is the photon trajectory with maximal angular momentum of the photon in $\kappa > 0$ case. In $\kappa > 0$ case, symmetric trajectories with $\pm a_0$ intersect while in $\kappa < 0$ case they do not. The straight lines are trajectories without angular momentum $L = 0$. The small blue circles are trajectories in $L \to \infty$ limit provided that $\kappa < 0$.

Now, let us consider the cases when either $\mathbf{T}$ or $\mathbf{L}$ become zero [they cannot be equal to zero simultaneously due to (15)]. If $\kappa < 0$ from Eq. (15) it follows that the only possibility is $L = 0$, $T \neq 0$, with T taking minimal value $T_{\min} = n_0/\lambda\!\!\!^{-}_0$. Using (17), (15) one can see that for $\kappa < 0$ one always has $|a_0| > 2r_0$ and for $\kappa > 0$ one has $R_0 > 2r_0$. So, in both cases there are not any ray closed trajectories inside the area of radius $2r_0$, see Fig. 2. In $\kappa > 0$ case, photons with angular momentum $L > L_{\max}$ will not form closed trajectories and correspondingly can not ensure perfect imaging and cloaking. This restriction is absent in $\kappa < 0$ case. In the conformal mapping scheme cloaking area is determined by the outer part of closed trajectories [2]. Therefore from (16), it follows that cloaking area will disappear for small L.

For $\kappa > 0$, $T = 0$, $L \neq 0$ angular mommentum L acquires the maximal value $L_{\max} = n_0 r_0/\lambda\!\!\!^{-}_0$ (15). As it follows from (14), when $T = 0$, $r^2 = 4r_0^2$, and $\mathbf{p} \perp \mathbf{r}$ the photon trajectory becomes a circle with the radius $R_0 = 2r_0$ and with center at $\mathbf{a}_0 = 0$ (see Fig. 2). In this state, the angular momentum of photon can be very large $n_0 r_0/\lambda\!\!\!^{-}_0 \gg 1$. These states are interesting for quantum information purposes [23]. Besides that, this state can be used as an optical resonator that is an accumulator of energy. To be convinced let us determine electric and magnetic fields on this trajectory. In geometrical optics one can use the following expansions [11]:

$$\mathbf{E} = e^{i\frac{\Psi}{\lambda\!\!\!^{-}_0}} \sum_{m \geqslant 0} (-i\lambda\!\!\!^{-}_0)^m \mathbf{e}_m \quad \mathbf{H} = e^{i\frac{\Psi}{\lambda\!\!\!^{-}_0}} \sum_{m \geqslant 0} (-i\lambda\!\!\!^{-}_0)^m \mathbf{h}_m, \tag{18}$$

where $\mathbf{e_m}, \mathbf{h_m}$ are functions of coordinates, which can be found by substituting expressions of $\mathbf{E}$ and $\mathbf{H}$ from (18) into Maxwell equations. Geometrical optics approximation corresponds to leading terms of expansion (18). The equation for eikonal Ψ has the form

$$n(\mathbf{r})\frac{d\mathbf{r}}{ds} = \nabla \Psi. \tag{19}$$

Substituting (9) into (19) and using (6) we then find

$$\Psi = \lambda\!\!\!^{-}_0 \mathbf{pr}. \tag{20}$$

As mentioned above, for this trajectory $T = 0$, $L = L_{\max} = n_0 r_0 k_0$, $\mathbf{p} \perp \mathbf{r}$, and $\mathbf{pr} \equiv 0$. Therefore on this trajectory, as it follows from (18), the phase (eikonal) remains constant during the round trip of the photon. Hence, in this state, photon constructively interferes with itself, and the energy is being accumulated (see also Refs. [24,25]). Note that the basic ray trajectory ($T = 0$, $L = L_{\max}$) with large angular momentum is similar to whispering gallery modes that originate as an eigenstate of dielectric sphere (see Ref. [26]).

Plasmon

In the $\kappa < 0$ case, the refraction index diverges at the point $r = 2r_0$. Such a situation can be realized, for example, on the metal surfaces near the plasmon resonance frequencies. Indeed, it is well known that dispersion equation of plasmon on the interface of a metal with dielectric constant $\varepsilon(\omega) < 0$

and with dielectric permittivity ε_d has the form

$$k_p = \frac{\omega}{c}\sqrt{\frac{\varepsilon(\omega)}{\varepsilon(\omega)+\varepsilon_d}}, \tag{21}$$

with $\varepsilon(\omega) \approx -\varepsilon_d$ near the plasmon resonance.

Suppose that the dielectric material has an inhomogeneous profile $\varepsilon_d \equiv \varepsilon_d(r)$. From the expression above, it can be presumed that a plasmon moves in a two-dimensional medium with refraction profile

$$n(r) = \sqrt{\frac{\varepsilon(\omega)}{\varepsilon(\omega)+\varepsilon_d(r)}}. \tag{22}$$

Suppose that $\mathbf{r}_p$ is a resonance point, $\varepsilon(\omega) = -\varepsilon_d(r_p)$. Expanding $\varepsilon_d(r)$ around r_p and assuming that $\varepsilon'(r_p) = 0$, we get

$$n(r) \approx \frac{1}{|r-r_p|}\sqrt{\frac{2\varepsilon(\omega)}{\varepsilon_d''(r_p)}}. \tag{23}$$

If we choose n_0 and r_0 such that

$$n_0 r_0 = \sqrt{\frac{2\varepsilon(\omega)}{\varepsilon_d''(r_p)}}, \quad \kappa < 0, \quad r_0 = \frac{r_p}{2}, \tag{24}$$

near the resonance point, $n(r)$ will obtain the form (1). So, it is possible to choose indexes $\varepsilon_p(r)$ such that near plasmon resonance point, closed trajectories and therefore cloaking phenomenon via conformal mapping can be realized (see also Ref. [27]).

Note that in the plasmon case because of the losses of electromagnetic field in metal [imaginary part of $\varepsilon(\omega)$] the refraction index of plasmon Eq. (23) acquires an imaginary part as well. Therefore our consideration is correct for those wavelengths and (noble) metals where this imaginary part is negligible.

IV. GENERALIZATIONS

In the previous section we related closed trajectories with the free particles on the sphere and two-sheet hyperboloid, which are the simplest three-dimensional maximally superintegrable systems. (The N-dimensional dynamical system is called maximally superintegrable when it has $2N-1$ functionally independent integrals of motion. In these systems all trajectories are closed). It was argued in Ref. [2] that the cloaking phenomenon takes place when all trajectories of the dynamical system defining the refraction index are closed. In other words, dynamical system should be maximally superintegrable. However, only the oscillator and the Coulomb problem on Euclidian spaces were considered in the mentioned paper. At the same time, there are their well-known generalizations to the spheres and two-sheet hyperboloids defined by the potentials [28]

$$V_{\rm osc} = \frac{\omega^2\mathbf{r}^2}{(1-\kappa\mathbf{r}^2)^2}, \quad V_{\rm Coul} = -\gamma\frac{|1-\kappa\mathbf{r}|}{r}, \tag{25}$$

as well as their further superintegrable deformations including, in particular, the Calogero-like term [15].

Considering the energy surface $\mathcal{H} - E = 0$ as a constraint (4) and properly rescaling the potential $V(\mathbf{r})$ along with value of energy E, one gets the modified profiles, which can be used for describing cloaking and perfect imaging phenomena

$$\mathcal{H} = (1+\kappa r^2)^2\mathbf{p}^2 + V(r), \quad \Rightarrow \quad \widetilde{n}(\mathbf{r}) = n_0\frac{\sqrt{|1-V(\mathbf{r})|}}{|1+\kappa\mathbf{r}^2|}. \tag{26}$$

The addition of Calogero-like term breaks spherical symmetry of the profile at the same time preserving its superintegrability. However, in this case symmetry algebra is highly nonlinear, which may cause troubles in the description of closed ray trajectories in a purely algebraic way.

Another way to find the profiles that should possess perfect imaging is to perform the simple canonical transformation $(\mathbf{p}, \mathbf{r}) \to (-\mathbf{r}, \mathbf{p})$. In this case the energy surface takes a form $|\mathbf{r}| = n(p)$. Then expressing p via r, we will get the new profile admitting cloaking, given by the function $\widetilde{n}_{\rm inv}$, which is inverse to the initial profile $n(r)$: $\widetilde{n}_{\rm inv}[n(r)] = r$. For example, it transforms the initial profile (1) to the one associated with the Coulomb problem

$$(1+\kappa p^2)^2 r^2 = \frac{n_0^2}{\lambda\!\!\!^{-}_0^2} \;\Rightarrow\; n_{\rm inv} = \sqrt{\frac{1}{\kappa}\left(\frac{n_0}{\lambda\!\!\!^{-}_0 r} - 1\right)}. \tag{27}$$

V. INCLUSION OF POLARIZATION

Let us briefly discuss the inclusion of polarization. To this end we should add to the Lagrangian the term $\mathbf{p}\dot{\mathbf{r}}$, the vector potential of Berry monopole $\mathbf{A}(\mathbf{p})\dot{\mathbf{p}}$, i.e., by the potential of the Dirac monopole located at the origin of the momentum space [18]

$$\frac{\partial}{\partial\mathbf{p}} \times \mathbf{A}(p) = \frac{\mathbf{p}}{|\mathbf{p}|^3}. \tag{28}$$

From the viewpoint of Hamiltonian formalism this means that we should preserve the form of the Hamiltonian (6) and replace the initial Poisson brackets (5) by the modified ones

$$\{f, g\} = \frac{\partial f}{\partial x_\alpha}\frac{\partial g}{\partial p_\alpha} - \frac{\partial f}{\partial p_\alpha}\frac{\partial g}{\partial x_\alpha} - \frac{s p_k}{p^3}\varepsilon_{klm}\frac{\partial f}{\partial x_l}\frac{\partial g}{\partial x_m}, \tag{29}$$

where s is the spin of the photon, which is equal to one for circularly polarized photon and to zero for linearly polarized photon. The above deformation of Poisson bracket violates the symmetry of the Hamiltonian, and therefore, can break the closed trajectories. However, the basic trajectory ($T = 0$, $L = L_{\rm max}$) in the limit $s \to 0$ preserves its form (see below). Using the new definition of the Poisson bracket Eq. (29), one gets the equations of motion in the form

$$\dot{\mathbf{r}} = \frac{\mathbf{p}}{p} + \frac{s\mathbf{L}}{\lambda\!\!\!^{-} r p^3}\frac{\partial n}{\partial r}, \quad \dot{\mathbf{p}} = \lambda\!\!\!^{-1}\nabla n(r) \quad \dot{\mathbf{T}} = \frac{2s\kappa\mathbf{L}}{\lambda\!\!\!^{-} r p^3}\frac{\partial n}{\partial r}(\mathbf{pr})$$
$$\dot{\mathbf{L}} = \frac{s}{\lambda\!\!\!^{-} r}\frac{\partial n}{\partial r}\left(\frac{\mathbf{p}(\mathbf{pr})}{p^3} - \frac{\mathbf{r}}{p}\right), \quad \dot{\mathbf{S}} = -\frac{s}{\lambda\!\!\!^{-} r}\frac{\partial n}{\partial r}\left(\frac{\mathbf{p}(\mathbf{pr})}{p^3} - \frac{\mathbf{r}}{p}\right), \tag{30}$$

where spin vector is determined as $\mathbf{S} = s\mathbf{p}/p$. When spin variable is taken into account in the spherical symmetrical

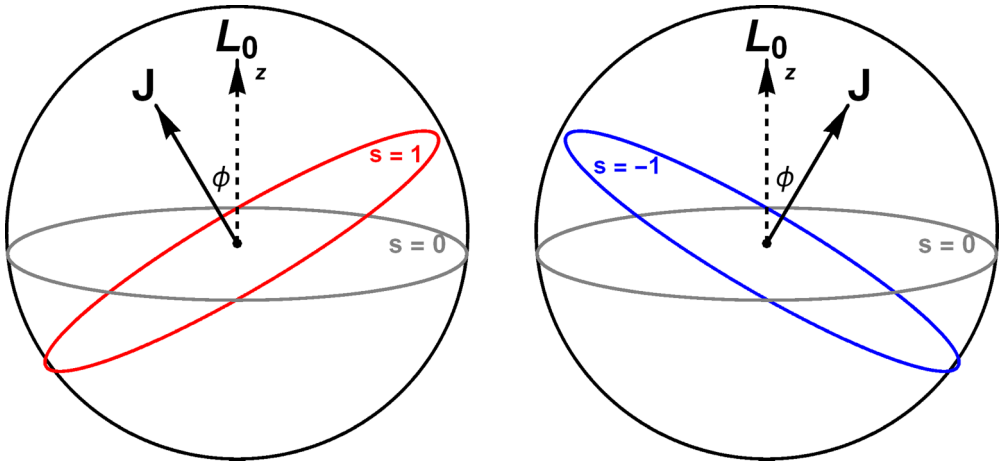

FIG. 3. Basic ray trajectories for photon with different polarizations. ϕ is the trajectory plane rotation angle.

refraction index profile $n(r)$, from Eq. (30) it follows that the total angular momentum $\mathbf{J} = \mathbf{L} + \mathbf{S}$ is preserved, $\dot{\mathbf{J}} \equiv 0$. We will develop perturbation theory on s exploring Eqs. (30). In the first-order perturbation theory on s, one can substitute all the terms containing s by their zero-order values (values when $s = 0$). Using this approach, we can see that, in the first-order approximation, the value of T on the basic trajectory is zero: $T(s) = 0$. Scalarly multiplying $\mathbf{J}$ by $\mathbf{r}$, for the basic trajectory, one gets $\mathbf{Jr} = 0$. In this approximation, it follows from Eq. (16) that $a_0 = 0$, $R = 2r_0$, and $|\mathbf{r}|^2 = 4r_0^2$. This means that basic trajectory remains a circle from the same sphere with the center at the origin. However, the plane of the circle is rotated and now is perpendicular to $\mathbf{J}$ and not to $\mathbf{L_0}$ as in $s = 0$ case. The rotation angle can be found by scalarly multiplying $\mathbf{J}$ and $\mathbf{p}$: $\mathbf{Jp} = sp$ and therefore $\cos\theta = s/J$ and $\sin\phi = s/J$, where θ and $\phi \approx \pi/2 - \theta$ are angles between $\mathbf{J}$ and $\mathbf{p}$ and $\mathbf{J}$ and $\mathbf{L_0}$, respectively (see Fig. 3).

In the first order on s, J can be substituted by $L_{\max} = n_0 r_0/\lambda$, $\sin\phi = s\lambda/n_0 r_0 \ll 1$. Hence the actual perturbation parameter is $s\lambda/n_0 r_0 \ll 1$ therefore perturbation theory can be applied for $s = \pm 1$ as well. The sign of rotation angle depends on the sign of s. So for right-hand circular polarized and left-hand circular polarized photons one will have different trajectories on the sphere. This is an analog of spin Hall effect [16–18] in Maxwell's fish eye refraction profile.

ACKNOWLEDGMENTS

Authors are grateful to Ashot Hakobian, Arsen Hakhoumian, Rubik Pogossian, and Khachik Nerkararian for useful discussions and comments. This work was performed within ICTP Affiliated Center program AF-04, and partial financial support from Armenian Committee of Science Grants No.18T-1C106 (A.N.) and No. 18T-1C082 (Zh.G.).

[1] J. Pendry, D. Schurig, and D. Smith, Science **312**, 1780 (2006).
[2] U. Leonhardt, Science **312**, 1777 (2006); New J. Phys. **8**, 118 (2006).
[3] Y. Lai, H. Chen, Zh.-Q. Zhang, and C. T. Chan, Phys. Rev. Lett. **102**, 093901 (2009).
[4] G. Gbur, Prog. Opt. **58**, 65 (2013).
[5] J. Zhou, T. Koschny, M. Kafesaki, E. N. Economou, J. B. Pendry, and C. M. Soukoulis, Phys. Rev. Lett. **95**, 223902 (2005).
[6] J. Sun, J. Zhou, and L. Kang, Opt. Express **16**, 17768 (2008).
[7] X. Chen, Yu Luo, J. Zhang, K. Jiang, J. B. Pendry, and S. Zhang, Nat. Commun. **2**, 176 (2011).
[8] H. Chen, B. Zheng, L. Shen, H. Wang, X. Zhang, N. I. Zheludev, and B. Zhang, Nat. Commun. **4**, 2652 (2013).
[9] J. S. Choi and J. C. Howell, Opt. Express **22**, 29465 (2014).
[10] J. C. Maxwell, Camb. Dublin Math. J. **8**, 188 (1854).
[11] M. Born and E. Wolf, *Principles of Optics*, 4th ed., (Pergamon Press, Oxford, 1970).
[12] U. Leonhardt, New J. Phys. **11**, 093040 (2009).
[13] U. Leonhardt and T. G. Philbin, Phys. Rev. A **81**, 011804(R) (2010).
[14] R. J. Blaikie, New J. Phys. **12**, 058001 (2010)
[15] T. Hakobyan, O. Lechtenfeld, and A. Nersessian, Phys. Rev. D **90**, 101701(R) (2014).
[16] M. Onoda, S. Murakami, and N. Nagaosa, Phys. Rev. Lett. **93**, 083901 (2004).
[17] K. Y. Bliokh, Avi Niv, V. Kleiner, and E. Hasman, Nat. Photon. **2**, 748 (2008).
[18] K. Bliokh, J. Opt. A: Pure Appl. Opt. **11**, 094009 (2009).
[19] Zh. Gevorkian, A. Hakhoumian, V. Gasparian, and E. Cuevas, Sci. Rep. **7**, 16593 (2017).
[20] Zh. Gevorkian, V. Gasparian, and E. Cuevas, Sci. Rep. **9**, 14053 (2019).
[21] P. A. M. Dirac, *The Principles of Quantum Mechanics*, 4th ed. (Clarendon, Oxford, 1958); A. Deriglazov, *Classical Mechanics: Hamiltonian and Lagrangian Formalism* (Springer, Berlin, 2010).
[22] Y. A. Kravtsov and Y. I. Orlov, *Geometrical Optics of Inhomogeneous Medium* (Springer, Berlin, 1990).

[23] M. Erhard, R. Fickler, M. Krenn, and A. Zeilinger, Light: Sci. Appl. **7**, 17146 (2018).
[24] O. Svelto, *Principles of Lasers*, 5th ed. (Springer, Berlin, 2010).
[25] K. Dadashi, H. Kurt, K. Ustun, and R. Esen, J. Opt. Soc. Am. B **31**, 2239 (2014).
[26] A. N. Oraevsky, Quantum Electron. **32**, 377 (2002).
[27] B. Baumeier, T. A. Leskova, and A. A. Maradudin, Phys. Rev. Lett. **103**, 246803 (2009).
[28] P. W. Higgs, J. Phys. A **12**, 309 (1979); H. I. Leemon, *ibid.* **12**, 489 (1979).